JOURNAL OF MATERIALS SCIENCE **36** (2001) 3649–3655

Valence compensated perovskite oxide system $Ca_{1-x}La_xTi_{1-x}Cr_xO_3$

Part II *Electrical transport behavior*

R. K. DWIVEDI
School of Materials Science and Technology, Institute of Technology, Banaras Hindu University, Varanasi—221 005, India

DEVENDRA KUMAR, OM PARKASH*
Department of Ceramic Engineering, Institute of Technology, Banaras Hindu University, Varanasi—221 005 (India).
E-mail: oparkash@banaras.ernet.in

Electrical transport behaviour of the valence compensated system $Ca_{1-x}La_xTi_{1-x}Cr_xO_3$ ($x \leq 0.50$) has been investigated by studying the Seebeck co-efficient, DC and AC conductivity as a function of temperature. Seebeck co-efficient, DC conductivity of different compositions has been measured in the temperature range 300 K–1000 K. AC conductivity for different compositions were determined in the temperature range 100–550 K and frequency range 10 Hz–10 MHz. Positive values of Seebeck co-efficient show that holes are the majority charge carriers. Conduction seems to occur by correlated barrier hopping of holes among Cr^{3+} and Cr^{4+} ions or $V_O^{\bullet}$ and $V_O^{\bullet\bullet}$. Almost equal values of activation energies obtained for DC conductivity and dielectric relaxation process show that both the processes occur by the same mechanism.

1. Introduction

Calcium titanate is a paraelectric material having orthorhombic structure at room temperature [1]. The structure becomes tetragonal at 600°C which changes to cubic at 1000°C. Study of optical density on the single crystal of $CaTiO_3$ has shown the band gap to be 3.4 eV at 0 K [2]. The electrical conductivity of this compound at 130°C, after exposing to oxidizing atmosphere, was found to be *p*-type [3]. $CaTiO_3$ can be converted to *n*-type semiconductor either by reduction at elevated temperature or by doping with donors [4]. The defect chemistry and electrical behavior at high temperature have been reported by many researchers including Chan and Smyth [5] and Balachandran and Eror [6–9]. Yttrium doped calcium titanate, when heated in an atmosphere of low partial pressure of oxygen, becomes semiconducting and exhibits relaxor behavior characteristic of barrier layers [4]. On replacing divalent calcium by trivalent yttrium or other rare earth ions, the charge neutrality is maintained by creating an appropriate number of vacancies on calcium sites [4, 8]. Lewis and Catlow [10] have reported that donor substitution on A-site will lead to the formation of titanium vacancies to maintain electrical charge neutrality. The acceptor dopants such as K^+ and Fe^{3+} will create oxygen vacancies [11]. During the last few years, some investigations on the electrical properties of valence compensated solid solution of alkaline earth titanates doped simultaneously and equivalently with La^{3+} or Y^{3+} on alkaline earth ion sites and Co^{3+}, Ni^{3+} on titanium sites have been made. These materials are found to exhibit interesting and useful dielectric properties [12–17].

We are reporting now the results of our investigations on an analogous system $Ca_{1-x}La_xTi_{1-x}Cr_xO_3$ which represents a valence compensated solid solution between $CaTiO_3$ and $LaCrO_3$ where calcium is replaced by lanthanum and titanium is replaced by chromium. The synthesis, structure and dielectric behaviour of these materials are communicated in Part–I of this series [18]. Compositions with $x \leq 0.10$ have been found to have orthorhombic structure similar (space group Pcmn) to $CaTiO_3$ while compositions with $x \geq 0.20$ have orthorhombic structure (space group Pbnm) similar to $LaCrO_3$. In the present paper the electrical transport behaviour of these materials is being reported. Such studies are useful in understanding the dielectric behaviour.

2. Experimental

The compositions with $x = 0.03, 0.05, 0.10, 0.20, 0.30$ and 0.50 in the system $Ca_{1-x}La_xTi_{1-x}Cr_xO_3$ were prepared by solid state ceramic method. The detailed method of preparation of these materials have been reported in part – I of this series of papers. For

* Author to whom all correspondence should be addressed.

measurement of Seebeck co-efficient, the sintered thick pellets (∼7–8 mm) were polished and pressed between two spring loaded platinum foils in a locally fabricated sample holder. The temperature of upper and lower surfaces of the pellet was measured by Pt/ Pt-10% Rh thermocouples welded to these foils. Thermo e.m.f. was measured using the Pt leads of the thermocouples employing KETHLEY 740 type Scanning Thermometer. Measurements were made at different steady temperatures and temperature gradients of 5–10°C were produced across the two surfaces of the pellets with the help of an auxiliary heating coil wrapped near the sample. DC conductivity was measured in the temperature range 500 K–1000 K at different steady temperatures using thin pellets (1–1.5 mm thick). AC conductivity was measured as a function of frequency in the temperature range 300 K– 550 K using 4192 - A Hewlett Packard Impedance Analyzer.

3. Results

3.1. Electrical conduction behavior

3.1.1. Seebeck co-efficient behavior

Plots of Seebeck coefficient, α (μV/K) vs. temperature in the temperature range 300 K–1000 K for all these samples are shown in Fig. 1. It is noted that all the compositions with $x \leq 0.50$ have positive values of α. α decreases with increasing temperature upto 400 K and thereafter it becomes almost temperature independent. The positive values of α indicate that these samples have p-type conductivity i.e. holes are the majority charge carriers. The values of Seebeck co-efficient at 500 K for various compositions are given in Table I. Both the end members of this perovskite solid solution system viz. $CaTiO_3$ and $LaCrO_3$ have been reported to exhibit p-type conduction. In $CaTiO_3$, p-type conduction is explained due to presence of excess acceptor impurities in the starting raw materials due to their more relative abundance in nature [19]. In $LaCrO_3$, some of Cr^{3+} ions transform to Cr^{4+} ions due to native impurities and the conduction is reported to occur by hopping of holes among Cr^{3+} and Cr^{4+} ions [20]. In the present system also, the conduction seems to be dominated by acceptor (chromium) ions as will be discussed in the next section, which explains the observed p-type behavior. ESR spectra of $Ca_{0.95}La_{0.05}Ti_{0.95}Cr_{0.05}O_3$ has shown that chromium is present in +3 state. It is in agreement with the observation of Mizushima *et al.* [21]. Presence of a small amount of Cr^{4+} is also not ruled out in these materials.

3.1.2. DC conductivity behavior

DC conductivity measurements have been made in the temperature range 500 K–1000 K. Plots of logarithm of dc resistivity, log ρ_{dc} with inverse of temperture for the compositions with $x = 0.05$, 0.10, 0.20, 0.30 and 0.50 are shown in Fig. 2. These plots are found to be linear obeying Arrhenius relationship:

$$\rho_{dc} = \rho_0 \exp \frac{E_a}{kT} \tag{1}$$

where E_a is the activation energy for conduction and k is Boltzmann constant. The value of activation energies of conduction determined by least square fitting of the resistivity data for various compositions are given in Table I. The value of DC resistivity at 500 K for various samples is also given in Table I. It is noted that the resistivity decreases as x increases from $x = 0.05$ to 0.10. The values of activation energy for these compositions are 0.33 and 0.37 eV respectively. The resistivity and the activation energy (0.43 eV) of the composition $x = 0.20$ is higher than that of $x = 0.10$. The resistivity and the activation energy decrease with increasing

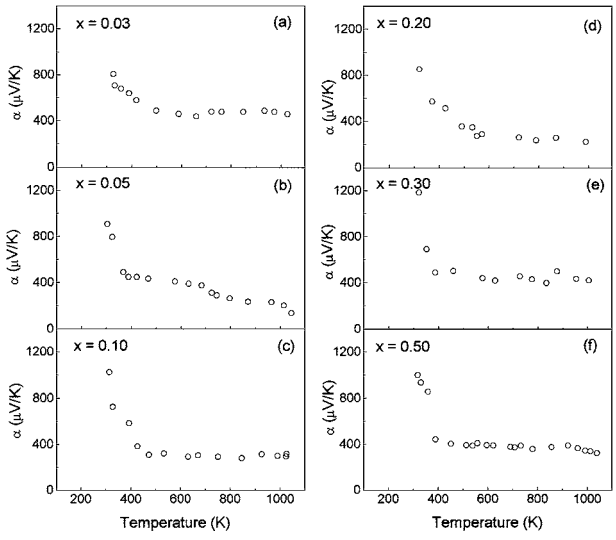

Figure 1 Plots of Seebeck co-efficient 'α' (μV/K) vs temperature (K) for various compositions in the system $Ca_{1-x}La_xTi_{1-x}Cr_xO_3$.

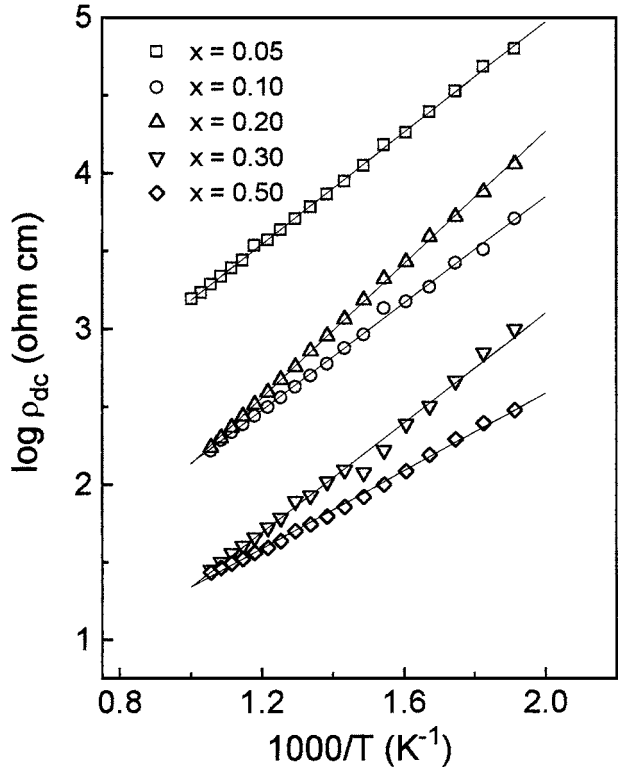

Figure 2 Variation of log ρ_{dc} with inverse of temperature for various compositions in the system $Ca_{1-x}La_xTi_{1-x}Cr_xO_3$.

TABLE I Values of activation energies, E_a Seebeck coefficeient 'α' and resistivity 'ρ_{dc}' for various compositions (x) in the system $Ca_{1-x}La_xTi_{1-x}Cr_xO_3$

Composition (x)	Activation energy* (ev) 400 K–550 K	Activation energy(DC) (ev) 550 K–1000 K	Seebeck co-efficient 'α'(μV/K) (500 K)	Resistivity 'ρ_{dc}' (ohm cm) (520 K)
0.05	0.19	0.37	489	6.30×10^4
0.10	0.27	0.33	441	1.15×10^4
0.20	0.38	0.43	372	5.09×10^3
0.30	0.29	0.34	491	9.91×10^2
0.50	0.24	0.27	407	3.10×10^2

*E_a is determined from log σ_{ac} at $\omega \to 0$ at different temperatures (extrapolating plateaus at various temperatures in log σ_{ac} vs log f plots)

x for $x > 0.20$. The anomalous change in resistivity around $x = 0.10$ may be correlated with the change in the structure around this composition. The crystal structure of the compositions with $x \leq 0.10$ is similar to that of $CaTiO_3$ whereas the structure of the compositions with $x \geq 0.20$ is similar to that of $LaCrO_3$ [18].

3.1.3. AC conductivity behavior

AC conductivity has been studied as a function of frequecy in the temperature range 100–550 K for all the compositions. Typical plots of log σ_{ac} vs log f at a few steady temperatures and log σ_{ac} vs 1000/T at 1, 10 and 100 kHz for $x = 0.05$ and 0.30 are shown in Figs 3 and 4 respectively. For $T \leq 200$ K, two plateaus separated by a frequency dispersion region are observed in log σ_{ac} vs log f plots of compositions with $x = 0.05$ and 0.10 (Figs. 3a). For $x = 0.20$, 0.30, and 0.50, the low frequency plateau is not observed for $T \leq 200$ K. However, for $T > 300$ K two plateaus separated by frequency dependent regions are seen in all these compositions. Thus the log σ_{ac} vs log f plots of these materials have three plateaus separated by frequency dependent regions. All the three plateaus do not appear at any temperature of measurement in any composition because of limited frequency range of measurement. The low frequency plateau for $x = 0.05$ and 0.10 at $T \geq 200$ K and for $x = 0.20$, 0.30, and 0.50 at $T \geq 300$ K represents the total conductivity whereas the high frequency plateau represents the contribution of grains to the total conductivity. The difference between these two represent the contribution of grain—boundaries to the overall conductivity. The low as well as high frequency plateaus observed in $x = 0.05$ and 0.10 for $T \leq 200$ K represent the two processes contributing to the bulk conduction behaviour. One of these processes relaxes in the high frequency region and contribution of the other process appears as a plateau in the high frequency region. The plateau corresponding to the total conductivity is not seen in these compositions at $T \leq 200$ K. The plateau corresponding to the total conductivity appears only above $T = 200$ K in these two compositions as mentioned above.

The frequency dependence of ac conductivity of the compositions $x = 0.05$ and 0.10 at low temperature and in the high frequency region (after first plateau), which corresponds to the relaxation of one of the bulk conduction processes, can be represented by

$$\sigma(\omega) \propto \omega^s \qquad (2)$$

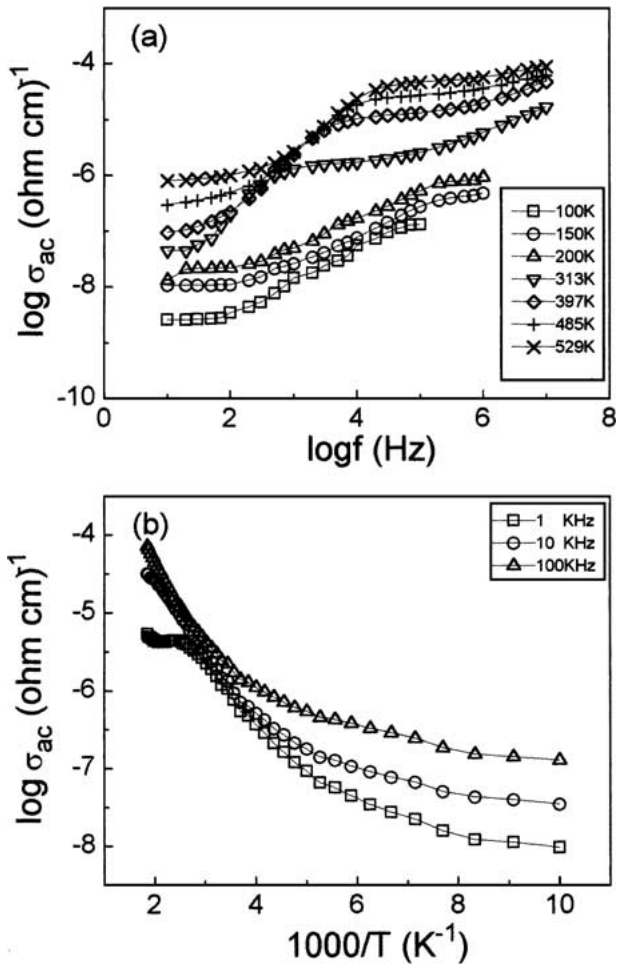

Figure 3 Variation of log σ_{ac} with (a) log f and (b) inverse of temperature for the composition $Ca_{0.95}La_{0.05}Ti_{0.95}Cr_{0.05}O_3$.

where the frequency dependence power exponent 's' is a weak function of frequency at a given temperature. The value of 's', found by least square fitting of the data of the frequency dependent region of log σ_{ac} vs log f plots in these compositions, lie in the range 0.50—1.0. The values of 's' decreases with increasing temperatures (Fig. 5). log σ_{ac} vs log f plots for all the compositions at $T \geq 300$ K have slope of nearly 1 corresponding to the relation $\sigma = \omega C_{GB}$ where σ and C_{GB} represent the total conductivity and capacitance of grain boundary respectively. This shows the switch over of grain-boundary process to the bulk conduction process. These results are similar to those observed by Vollmann *et al.* [22] in acceptor doped $SrTiO_3$.

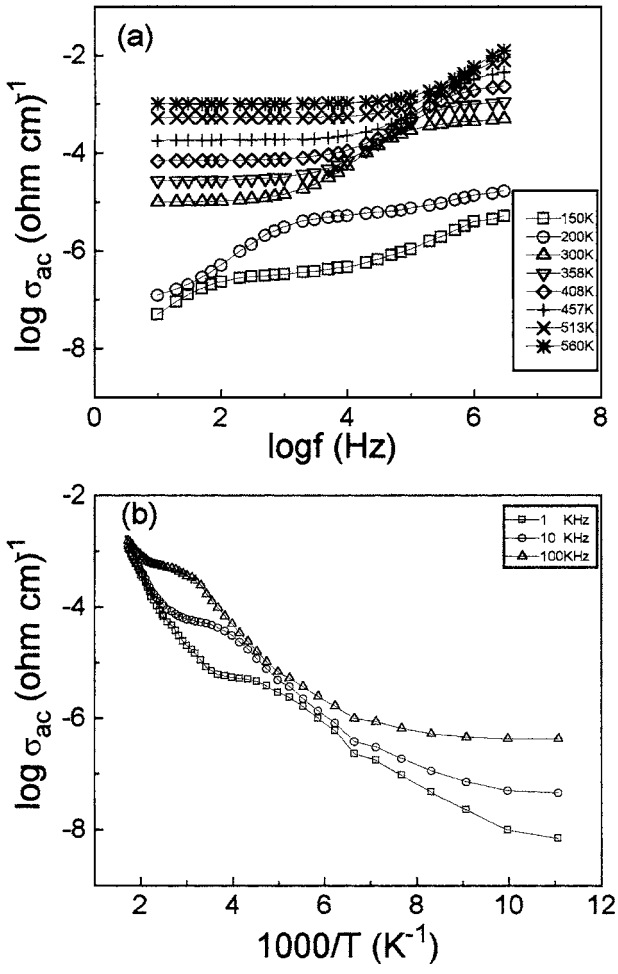

Figure 4 Variation of log σ_{ac} with (a) log f and (b) inverse of temperature for the composition $Ca_{0.70}La_{0.30}Ti_{0.70}Cr_{0.30}O_3$.

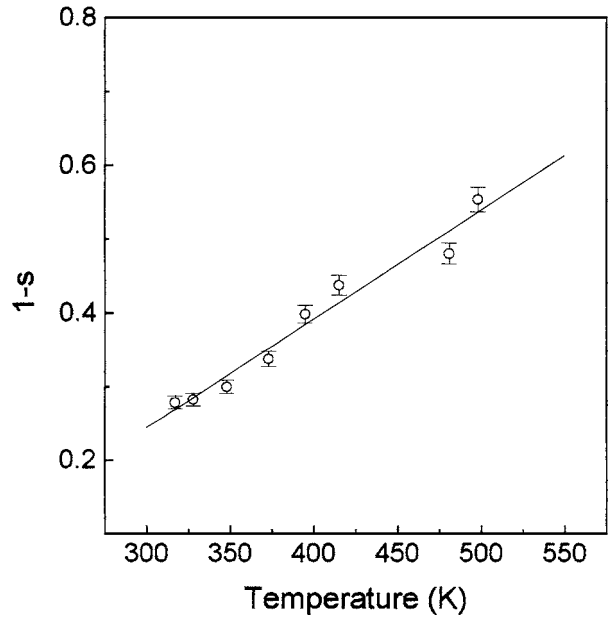

Figure 5 Plot of '1-s' vs temperature for composition $Ca_{0.90}La_{0.10}Ti_{0.90}Cr_{0.10}O_3$.

In the log σ_{ac} vs log f plots of these samples, Figs 3a and 4a, the low frequency plateau in the high temperature region i.e. for $T \geq 300$ K for $x = 0.05$ and 0.10 and for $T \geq 200$ K for $x = 0.20$, 0.30 and 0.50, corresponds to total conductivity due to grains and grainboundaries and the high frequency plateau at the higher temperatures corresponds to the bulk conductivity. The values of conductivity of grains and grainboundaries at different temperatures can be obtained from these plots. Vollmann *et al.* [22] did not report the third plateau region in their log σ_{ac} vs log f plots which was observed in the present system because their electrical conductivity data were recorded in the high temperature region ($T > 400$ K). In this temperature range, the possibility of bulk conduction relaxation is negligible. In our system, the electrical conductivity data were recorded upto low temperature (i.e. 100 K). Hence due to relaxation of one frequency dependent conduction process, the third plateau is observed at very low temperature of observation.

4. Discussion

Calcium titanate is a wide band gap i.e. 3.2–3.4 eV material [2–3, 23]. In $CaTiO_3$ the oxygen 2p orbitals form the valence band, which is separated from the conduction band, formed from 4s levels of titanium ions. The electrical properties of alkaline earth titanates (ABO_3) have been widely investigated [24–29]. The electrical transport in these materials depends on the charged defects whose concentration depends on doping level and processing parameters. These materials may lose oxygen at high temperature (>1000°C) in accordance with the reaction:

$$O_0 \Leftrightarrow \frac{1}{2}O_2 + V_0^{\bullet\bullet} + 2e' \tag{3}$$

These oxygen vacancies are doubly positively charged at high temperature. Below ~550°C, oxygen vacancies exist as singly ionized defects as $V_0^{\bullet}$ [30–31] according to the reaction

$$V_0^{\bullet\bullet} + e' \Leftrightarrow V_0^{\bullet} \tag{4}$$

Oxygen vacancies remain singly ionized upto 4 K, below which they exist as neutral species. These oxygen vacancies act as intrinsic donors. The trivalent ions substituted at A sites and pentavalent ions at B sites (La^{3+} and Nb^{5+} separately) act as extrinsic donors [$D^{\bullet}$]. These donors have very little ionization energy and exist mostly in fully ionized state around and above room temperature [32]. Cation (M or Ti) vacancies are predominant intrinsic acceptors in the alkaline earth titanates [33–37]. Trivalent ions A^{3+} on Ti^{4+} site, deliberately added act as extrinsic acceptors. They ionize as

$$A_{Ti}^{x} \Leftrightarrow A' + h^{\bullet} \tag{5}$$

Besides the above defects, electrons and holes may be generated intrinsically by excitation across the band gap as

$$O \Leftrightarrow e' + h^{\bullet} \tag{6}$$

The overall charge neutrality condition requires that the sum of charges on the positively and negatively

charged defects should be equal, viz.

$$n + 2[V''_M] + [V'_M] + [A'] = p + 2[V_0^{\bullet\bullet}] + [V_0^{\bullet}] + [D^{\bullet}] \quad (7)$$

The square brackets indicate the concentration and the number outside the brackets indicates the charge on the defect species.

The above equation can be simplified by considering only the predominant defects under different prevailing conditions i.e. temperature, partial pressure of oxygen and concentration of dopants. The electrical conductivity depends on the concentration of charge carriers i.e. e', $h^{\bullet}$ and $V_O^{\bullet\bullet}$ and their mobilities (μ_e, μ_h and $\mu_{V_O^{\bullet\bullet}}$) assuming that mobilities of the cations in the perovskites is very small as compared to electrons/holes or oxygen vacancies.

$$\sigma = ne\mu_e + pe\mu_h + 2e[V_0^{\bullet\bullet}]\mu_{V_0^{\bullet\bullet}} \quad (8)$$

In the high temperature region, the titanate samples equilibrate with the ambient oxygen in air according to the equation (3.4) rapidly within reasonable period of time. In acceptor doped and undoped titanate ceramics, oxygen vacancies are predominant ionic defects. The kinetics of attaining equilibrium with ambient oxygen is determined by their high ambipolar diffusion coefficient. It takes only a few minutes to attain a new equilibrium after a sudden change in Po_2 at 1000°C [29]. In the low temperature region, the oxygen equilibration is far too slow to be effective in the time scale of measurement. Therefore, the concentration of oxygen vacancies can be regarded as frozen in. The transition range from high temperature to low temperature depends on the sample thickness, grain size, the rate of cooling and the nature of grain boundary barriers for the cross transport of oxygen vacancies. For alkaline earth titanates, this temperature range extends from 750 K to 950 K [28]. There may be contribution of ionic conductivity in these materials due to non-associated frozen in oxygen ion vacancies:

$$\sigma_{V_0^{\bullet\bullet}} = 2e[V_0^{\bullet\bullet}]\mu_{V_0^{\bullet\bullet}} \quad (9)$$

$$\sigma_{V_0^{\bullet}} = e[V_0^{\bullet}]\mu_{V_0^{\bullet}} \quad (10)$$

The mobilities $\mu_{V_O^{\bullet\bullet}}$ or $\mu_{V_O^{\bullet}}$ are thermally activated. The activation energy for the diffusion of doubly ionized oxygen vacancies in alkaline earth titanates is approximately 1.0 eV [38].

The observed values of activation energies for dc conduction for various compositions in the system $Ca_{1-x}La_xTi_{1-x}Cr_xO_3$ are in the range 0.30 – 0.40 eV. This rules out the possibility of intrinsic conduction and conduction due to migration of oxygen ion vacancies. The +ve values of Seebeck co-efficient, α indicate that the holes are the majority charge carriers. In all these samples, α decreases with increasing temperature upto 400 K. Thereafter it remains constant. The constant values of Seebeck co-efficient in the temperature range 500–1000 K show that the number of charge carriers remains constant in this range. The decrease in the resistivity of these samples with increasing temperature above 500 K is therefore due to thermally activated mobility of charge carriers.

In this velence compensated system $Ca_{1-x}La_xTi_{1-x}Cr_xO_3$, lanthanum La^{3+} and chromium Cr^{3+} ions are substituted for Ca^{2+} and Ti^{4+} in equivalent amount for internal charge compensation respectively. It has been reported that for small concentration of lanthanum ions, the charge is compensated electronically according to

$$[La_{Ca}^{\bullet}] = n \quad (11)$$

while at higher concentration of lanthanum, the charge compensation may occur by calcium or titanium ion vacancies [4, 39]:

$$[La_{Ca}^{\bullet}] = 2[V''_{Ca}] \text{ or } 4[V'''_{Ti}] \quad (12)$$

In the former case, the conduction is n-type and the conductivity should increase with increasing lanthanum concentration. In the case of ionic compensation, the conductivity is not expected to increase much due to low mobilities of cation vacancies in the temperature range of measurement. We observe p-type conduction in this system and the conductivity increases with increasing x. This shows that conduction is mainly influenced by chromium ions. Lanthanum ions on calcium sites in these samples are compensated by chromium ions on titanium, Ti^{4+} sites but a small amount may be compensated by cation vacancies whereas chromium ions on titanium sites are mainly compensated by lanthanum ions on calcium sites and traces may be compensated by holes. This is due to inefficient mixing of the component salts in the ceramic method used for the preparation of these materials. Compositions with small concentration of dopants ($x \leq 0.03$ or so) are more chemically inhomogeneous as compared to compositions with higher concentration due to this. Therefore, in compositions with small values of x, there seems to be electronic compensation significantly in local regions. At low values of x, the electrons generated by ionization of La^{3+} ions will compensate the holes, which are present because of excess concentration of acceptor impurities in the starting raw materials to a large extent. The properties are therefore dominated by ionization of chromium ions on Ti^{4+} sites, which gives holes. With increasing x, the internal charge compensation and ionic compensation in local regions due to inhomogeneous mixing occurs predominantly. The positive values of α observed in these materials is in conformity with this. The holes, present in this system, are present as Cr^{4+} ions. The dc conduction occurs by activated hopping of charge carriers among Cr^{3+} and Cr^{4+} ions on Ti^{4+} sites [40]. Decreasing values of frequency dependence exponent 's' with increasing temperature (Fig. 5) shows that conduction occurs due to correlated barrier hopping of charge carriers as discussed earlier. The conduction due to hopping of small polarons is ruled out as log σT vs 1/T plots are not linear [40]. Further, for hopping of small polarons 's' should increase with temperature which is contrary to our observation.

It has been discussed above that electrical conduction characteristics of different compositions in this valence compensated system are dominated by acceptor chromium Cr^{3+} ions. The ac electrical characteristics ($\log \sigma_{ac}$ vs $\log$ f plots) of these compositions are similar to the acceptor doped titanates having high insulation resistance because grain boundaries act as a highly resistive barriers for cross transport of charge carriers [29]. The grain boundary barriers are caused by grain boundary states that are oppositely charged as compared to the background dopant centres in the bulk. This causes a depletion of mobile carriers in the vicinity of grain boundaries. The grain boundary depletion space charge layers are described as back to back double Schottky barriers. The width of the grain boundary space charge layer depends on the acceptor concentration, the temperature and oxygen partial pressure during firing. Vollmann and Waser [41] represented the ceramic samples by brick wall model. In this model the ceramic corresponds to an electrical network consisting of two parallel *R-C* circuits connected in series. One of these *RC* element corresponds to the bulk and the other to the grain boundaries contribution. For such an equivalent circuit, representing the ceramics, two plateaus are observed in $\log \sigma_{ac}$ vs $\log$ f plots. The plateau in the low frequency range gives the total conductivity of the sample while the high frequency plateau gives the bulk conductance. The two plateaus are separated by a frequency dependent region having a slope 1.

In the present system, two plateaus connected by a frequency dependent region are observed in all the compositions at $T \geq 300$ K. The high frequency plateau, observed at low temperatures is only observed in $x = 0.05$ and 0.10 for $T \leq 300$ K. This gives the contribution of one bulk process, which does not relax in the highest frequency available at these temperatures. The low frequency plateau at low temperatures in these samples corresponds to the total conductivity of both the bulk processes. The low frequency plateau, appearing at $T \geq 300$ K in all the samples, corresponds to the total conductivity (including grains as well as grain boundaries).

It follows from the frequency dependence of AC conductivity and dielectric behavior (communicated in part – I) [18] that there are three contributions to the overall electrical/dielectric behavior. The contribution which appears in the high temperature ($T \geq 300$ K in all the samples) and low frequency region is due to interfacial space charge polarization present at grains—grain boundaries interfaces. Its time constant, *RC* is large due to large values of R and C. R decreases with increasing temperature and its contribution appears as a small arc in the low frequency region in the complex plane modulus plots (to be discussed in part III of this series). The capacitance associated with this contribution is in the nano-farad range. This order of capacitance is assigned to thin regions like grain boundaries interfaces [42]. This contribution appears only above a certain temperature. This is because at lower temperatures, the dc conductivity due to long range movement of the charge carriers is small. It increases exponentially with temperature. Therefore, with increasing temperature, these charge carriers can move easily through the bulk get intercepted at the grain-boundaries, which act as barriers for their cross transport. This has already been mentioned. This trapping of charge carriers at grain-boundaries gives rise to space charge polarization. This is manifested by a rapid rise in dielectric constant with temperature in the high temperature range. This contribution of space charge polarization is clearly seen in ε_r vs $\log$ f plots of compositions with $x = 0.20$ and 0.30 in the intermediate frequency region [18]. The relaxation seems to be similar to the Debye relaxation process. The resistive part of this contribution can be obtained from the difference in the resistance corresponding to low frequency plateau and high frequency plateau observed in $\log \sigma_{ac}$ vs $\log$ f plots for all the compositions.

Debye type peaks are observed in D vs T or D vs $\log$ f plots of all the compositions [18]. These peaks are observed only at certain temperatures in the frequency range of measurements. This may be due to the orientational polarization present in the bulk. These materials contain a variety of defects viz. $V_O^{\bullet}$, $V_O^{\bullet\bullet}$, $La_{ca}^{\bullet}$, V'_{ca}, V''_{ca},$Cr_{Ti^{4+}}^{3+\prime}$, $Cr_{Ti^{4+}}^{4+}$. Oxygen vacancies exist predominatly in singly ionized state $V_0^{\bullet}$ upto (550°C) above which they change into doubly ionized state. But these materials contain some frozen in doubly ionized oxygen vacancies at low temperatures [29, 43]. These positively charged defects might be associated to from dipoles of the type $Cr_{Ti}^{3+\prime}$ - $V_0^{\bullet}$ or $2Cr_{Ti}^{3+\prime}$ - $V_0^{\bullet\bullet}$. These dipoles can change orientation due to hopping of holes among Cr_{Ti}^{x} and Cr'_{Ti} sites. Another process, which may occur is the hopping of holes among $V_0^{\bullet}$ and $V_0^{\bullet\bullet}$ which will again lead to change in orientation of dipoles. The values of activation energies calculated from the Arrhenius plots of relaxation times vs temperature ($\log \tau$ vs $1000/T$) in low temperature range (200–350 K) and in high temperature range (350–550 K) are found to be around 0.10 eV and 0.25 eV respectively. These values agree with the values obtained from Arrhenius plots of conductivity obtained from the plateau regions of $\log \sigma_{ac}$ vs $\log$ f plots in the same temperature regions. This shows that both the polarization and conduction occur due to the same process. DC conductivity should increase with increasing x. If the conduction is dominated by the chromium ions as proposed. With increasing x, the probability of formation of associated pairs such as Cr'_{Ti} - $V_O^{\bullet}$ or Cr'_{Ti} - $V_O^{\bullet\bullet}$ - Cr'_{Ti} also increase leading to trapping of the holes. It is because of these competing processes that there is no definite trend of σ_{dc} with x. At higher temperatures, when these defect pairs are dissociated freeing the trapped charge carriers sites, increase in conductivity with increasing x is observed as expected.

Nowick *et al*. [44] observed dielectric relaxation peaks at low temperatures in acceptor doped potassium tantalate and calcium titanate. They determined the activation energies for this relaxation process and found these in the range 0.10–0.40 eV. They ascribed this relaxation to orientational polarization arising due to formation of associated defects of the type M''_{Ta} - $V_O^{\bullet\bullet}$, M''_{Ti} - $V_O^{\bullet\bullet}$ where M represents trivalent or divalent acceptor on Ta or Ti sites. The change in orientation of dipoles occurs due to jumping of $V_0^{\bullet\bullet}$ in Ti(O_5 - $V_0^{\bullet\bullet}$)

octahedra. They explained low values of activation energies due to sufficient readjustment of ions around the impurity atoms (acceptor dopants) which ease the jumping of oxygen ions with low value of activation energy. This mechanism is ruled out in our samples as this will not contribute to DC conductivity.

Conduction in these samples seems to occur by hopping of holes among Cr^{3+} - Cr^{4+} sites and among $V_0^{\bullet}$ - $V_0^{\bullet\bullet}$ pairs. This is clearly reflected in the two plateaus, observed in log σ_{ac} vs log f plots of $x = 0.05$ and 0.10 at low temperatures ($T \leq 200$ K) (Figs 4a and 5a). The higher activation energies observed in high temperature region (Table III) in these samples may be due to the presence of defect pairs such as Cr'_{Ti} - $V_O^{\bullet}$ which trap the charge carriers. With increasing temperature, these defect pairs will dissociate making these hopping sites available for conduction. Therefore the activation energy for conduction in high temperatue region will include the dissociation energies of these pairs in addition to activation energy for migration of charge carriers. This explains the higher values of activation energies of conduction as compared to low temperature values.

5. Conclusions

Seebeck coefficient is found to be positive over the entire temperature range of measurement showing that holes are the majority charge carriers. Measurement of DC and AC conductivity shows that at low temperature conduction occurs due to thermally activated rotation of dipoles in a process similar to Debye relaxation. With increasing temperature conduction seems to occur by thermally activated hopping of charge carriers among $V_O^{\bullet}$ - $V_O^{\bullet\bullet}$ and Cr^{3+} and Cr^{4+} sites.

Acknowledgments

Financial support from Department of Science and Technology, Government of India is gratefully acknowledged. We are very grateful to Prof. T. K. Gundurao, I. I. T., Powai, Mumbai for ESR measurements.

References

1. H. F. KAY and P. C. BAILEY, *Acta. Cryst.* **10** (1957) 219.
2. A. LINZ and K. HERINGTON, *J. Chem. Phys.* **28** (1958) 824.
3. G. A. COX and R. H. TREDGOLD, *Br. J. Appl. Phys.* **18** (1967) 37.
4. S. NEIRMAN and I. BURN, *J. Mater. Sci.* **19** (1984) 737.
5. N. H. CHAN and D. M. SMYTH, *J. Electrochem. Soc.* **123** (1976) 1584.
6. U. BALACHANDRAN and N. G. EROR, *J. Mater. Sci.* **17** (1982) 1207.
7. *Idem.*, *ibid.* **17** (1982) 1795.
8. *Idem.*, *J. Phys. Chem. Solids* **44** (1983) 231.
9. *Idem.*, *J. Mater. Sci.* **23** (1988) 2676.
10. G. V. LEWIS and C. R. A. CATLOW, *J. Phys. Chem. Solids* **47** (1986) 89.
11. B. JAFFE, J. W. R. COOK and H. JAFFE, "Piezoelectric Ceramics, Chap. 5" (Academic Press New York, 1971).
12. OM PARKASH, L. PANDEY and DEVENDRA KUMAR, *J. Alloys and Compounds* **206** (1994) 147.
13. CH. D. PRASAD, Ph.D. Thesis, Banaras Hindu University, Varanasi, India, 1988.
14. D. KUMAR, CH. D. PRASAD and OM PARKASH, *J. Phys. Chem. Solids* **51** (1990) 73.
15. H. S. TEWARI, Ph.D. Thesis, Banaras Hindu University, Varanasi, India, 1994.
16. OM PARKASH, H. S.TEWARI, V. B. TARE and D. KUMAR, *J. Phys. D; App. Phys.* **26** (1993) 676.
17. OM PARKASH, CH. D. PRASAD and D. KUMAR, *ibid.* **27** (1994) 1509.
18. R. K. DWIVEDI, DEVENDRA KUMAR and OM PARKASH, *J. Mat. Sci.* (Communicated).
19. D. M. SMYTH, *Prog. Solid. State Chem.* **15** (1984) 145.
20. G. V. S. RAO, B. N. WANKLYN and C. N. R. RAO, *J. Phys. Chem. Solids.* **32** (1971) 345.
21. K. MIZUSHIMA, M. TANAKA and S. IIDA, *J. Phys. Soc. Jpn.* **32** (1972) 1519.
22. M. VOLLMANN, R. HAGENBECK and R. WASER, *J. Am. Ceram. Soc.* **80** (1997) 2301.
23. L. A. HARRIS and R. H. WILSON, *Ann. Rev. Mater. Sci.* **8** (1978) 99.
24. J. DANIELS and K. H. HARDTL, *Philips Res. Rep.* **31** (1976) 487.
25. N. G. EROR and U. BALACHANDRAN, *J. Solid State Chem.* **42** (1982) 227.
26. N. H. CHAN, R. K. SHARMA and D. M. SMYTH, *J. Am. Ceram. Soc.* **64** (1981) 556.
27. *Idem.*, *J. Electrochem. Soc.* **128** (1981) 1762.
28. R. WASER, *J. Am. Ceram. Soc.* **74** (1991) 1934.
29. R. MOOS and K. H. HARDTL, *ibid.* **80** (1997) 2549.
30. R. MOOS, W. MENESKLOU and K. H. HARDTL, *Appl. Phys.* **A 61** (1995) 389.
31. C. LEE, J. DESTRY and L. J. BREBNERC, *Phy. Rev.* **B11** (1975) 2299.
32. R. MOOS, Ph.D. Thesis, University of Karlsruhe, Germany, 1994.
33. T. Y. TIEN and F. A. HUMMEL, *Trans. Br. Ceram. Soc.* **66** (1967) 233.
34. N. G. EROR and U. BALACHANDRAN, *J. Solid State Chem.* **40** (1981) 85.
35. H. M. CHAN, M. P. HARMER and D. M. SMYTH, *J. Am. Ceram. Soc.* **69** (1986) 507.
36. D. MAKOVEC, Z. SAMARDZIJA, U. DELALUT and D. KOLAR, *ibid.* **78** (1995) 2193.
37. W. MENESKLOU, Ph.D. Thesis, University Karlsruhe, Karlsruhe, FRG, 1996.
38. A. E. PALADINO, *J. Am. Ceram. Soc.* **48** (1965) 476.
39. R. E. NEWNHAM, *J. Mater Educ.* **5** (1983) 941.
40. D. P. KARIM and A. T. ALDRED, *Phys. Rev.* **B20** (1979) 2255.
41. M. VOLLMANN and R. WASER, *J. Am. Ceram. Soc.* **77** (1994) 235.
42. I. H. HODGE, M. D. INGRAM and A. R. WEST, *J. Electroanal. Chem.* **74** (1976) 125.
43. R. MOOS and K. H. HARDTL, *J. Appl. Phys.* **80** (1996) 393.
44. A. S. NOWICK, S. Q. FU, W. K. LEE, B. S. LIM and J. SCHERBAN, *Materials Science Engg.* **B23** (1994) 19.

Received 28 March 2000
and accepted 6 February 2001